*Polish Journal of Chemical Technology, 10, **1**, 60 — 65, 2008, 10.2478/v10026-008-0015-5*

Size-dependent growth kinetics of vitamin C crystals in water solutions of L(+)-ascorbic acid with the addition of methanol and ethanol

[1]Bogusława Wierzbowska, [2]Krzysztof Piotrowski, [1]Joanna Koralewska, [1]Andrzej Matynia

[1]Wrocław University of Technology, Faculty of Chemistry, Wybrzeże Wyspiańskiego 27, 50-370 Wrocław, Poland, e-mail: andrzej.matynia@pwr.wroc.pl
[2]Silesian University of Technology, Department of Chemical & Process Engineering, ks. M. Strzody 7, 44-101 Gliwice, Poland, e-mail: krzysztof.piotrowski@polsl.pl

Growth kinetics of vitamin C crystals during the batch mass crystallization process in L(+)-ascorbic acid – methanol – ethanol – water system was determined. The linear growth rate values were estimated on the basis of the product crystal size distributions. The kinetic model of the continuous process in a MSMPR crystallizer was adopted for the batch mode description according to Nyvlt's conception, taking the size-dependent growth (SDG) rate effects into consideration. The kinetic parameter values were determined with a Rojkowski hyperbolic SDG model. A good compatibility between the experimental product crystal population density distributions and the SDG model predictions was observed. The interpretation of the kinetic data was presented and discussed.

Keywords: vitamin C, methanol, ethanol, batch cooling crystallizer, crystals growth rate, size-dependent growth (SDG) kinetics.

INTRODUCTION

Vitamin C (L(+)-ascorbic acid, denoted later in the text as LAA) for the medical needs is synthesized from D-glucose[1, 2], the most often, according to Reichstein, procedure[3]. Raw, technical-grade vitamin C (96 – 98 mass % of LAA) should be purified by mass crystallization from its water solutions[4, 5], usually in a multistage batch regime[6 – 12]. An introduction into this physicochemical system an additional, third constituent – methanol or ethanol – influences all the partial phenomena, forming together the mass crystallization process[13 – 15]. Under these new conditions the process yield increases, product crystals quality improves while a number of crystallization stages reduces[16 – 19].

Taking into consideration all these advantageous aspects of alcohol(s) presence some new technological concepts, focused on the optimization of the batch mass crystallization process of LAA in a four-compound system: LAA – MeOH – EtOH – H_2O, were developed. It was found, that both these alcohols substantially and advantageously influence the solubility and nucleation of LAA[20 – 22], crystals growth[23], their quality[24] as well as the general process yield[25]. The growth kinetics of LAA crystals, representing all these effects indirectly, was roughly estimated by analyzing the product crystal size distributions[26]. The calculation results – effects of adopting the most simplified model of a continuous mass crystallization process kinetics in a theoretical MSMPR (*Mixed Suspension Mixed Product Removal*) crystallizer for the batch mode description, according to a Nyvlt's conception, is presented in the authors' work[27]. This model, assuming G(L) = const. (*Size-Independent Growth* – SIG kinetics) is, however, not adequate to correctly reflect the experimentally detected, characteristic initial curvature of the population density distribution in a coordinate system lnn(L) – L within the range of the smallest-size crystals (of L < 100 μm). Taking this fact into account in the presented work, the research results, with their kinetic interpretation (G(L) ≠ const. indicating *Size-Dependent Growth*, SDG, phenomena), making allowance for the intrinsic nonlinearity of the population density course in a lnn – L coordinate system, are presented.

EXPERIMENTAL

Setup and procedure

The research tests were performed in a laboratory batch crystallizer of the DT (*Draft Tube*) type with the inner circulation of suspension of V_w = 0.6 dm^3 working volume, equipped with a propeller mixer. A detailed scheme of a computer-controlled laboratory test stand, as well as the experimental procedure applied, are presented in the authors' other works[20, 27]. The crystallizer volume was filled with the solution of the initial composition selected from the ones shown in Table 1. In this Table there are also presented the data characterizing the solubility[20], the batch process time, the metastable zone width[20], as well as the product-crystals quality[24] resulting from the cooling of these selected solutions (assuming the constant cooling rate, $R_T = 8.33 \cdot 10^{-3}$ K s^{-1}) down till the final temperature T_f = 283 K is attained (additional „post-process" time t_f = 900 s was applied for the stabilisation of the product suspension under final conditions).

Table 1. The influence of the initial composition of batch solution on the parameters of the crystallization of L(+)-ascorbic acid in a batch cooling DT crystallizer and the resulting product crystals properties (LAA - MeOH - EtOH - H_2O system)

Specification	Solution		
	1	2	3
Initial concentration in the solution, mass %, of:			
– L(+)-ascorbic acid	40	45	50
– methanol	10	10	10
– ethanol	10	10	10
– water	40	35	30
Solubility temperature T_s, K	335	343	353
Nucleation temperature T_{cr}, K	306	321	335
Critical supercooling ΔT_{max}, K	29	22	18
Crystallization time t_{cr}, h	1.02	1.52	1.98
Crystal characteristic:			
– mean size L_m, μm	214	339	448
– coefficient of variation CV, %	62.2	46.7	31.0

The cooling rate: $R_T = 8.33 \cdot 10^{-3}$ K s^{-1}
The final temperature of the crystallization: T_f = 283 K

For the calculation of the crystals linear growth rate, G, an indirect method was applied, based on the theoretical analysis of the population density distribution of crystals produced in a batch crystallizer with a programmed cooling mode (unsteady state conditions resulting in a complex batch polythermal process of coupled nucleation and crystals growth[28, 29]). It should be noted that it is not a strictly precise method since it adopts a kinetic model of a continuous mass crystallization process in a MSMPR[30, 31] crystallizer, directly to the batch conditions. The theoretical grounds for this adaptation, as well as the theoretical aspects of the resulting kinetic data interpretation are presented in other authors' work[27].

The product-crystal size distributions were obtained with the use of the particle laser analyzer COULTER LS-230. The individual population density values, n_i, were calculated from the mass m(L) (or volume, V(L)) the size distribution data according to the formula presented below, Equation (1):

$$n_i = \frac{m_i}{k_v \rho L_i^3 \Delta L_i V_w} = \frac{V_i}{k_v L_i^3 \Delta L_i V_w} \tag{1}$$

RESULTS

Size-dependent growth kinetics

The resulting population density courses of LAA crystals produced from the assumed batch solutions (see Table 1) are presented in Figure 1. It results from this figure that in a lnn(L) – L coordinate system for the crystals of the L < 100 μm size, the experimentally determined population density distributions are concave to top. This specific shape can be interpreted as an evidence of a more complex intrinsic kinetics of crystals growth than it can result from the most simplified SIG model[27]. In particular, this type of population density distribution can result from the occurrence of size-dependent growth phenomena (SDG) or/and growth rate dispersion (G_i = const., *Growth Rate Dispersion* – GRD)[31]. It should be noted that both these phenomena (SDG and GRD) are undistinguishable while considering only the population density distribution data, thus for engineering calculation purposes both phenomena can be treated as an integrity (both producing identical external effect) and a subject of description by a more mathematically convenient SDG model.

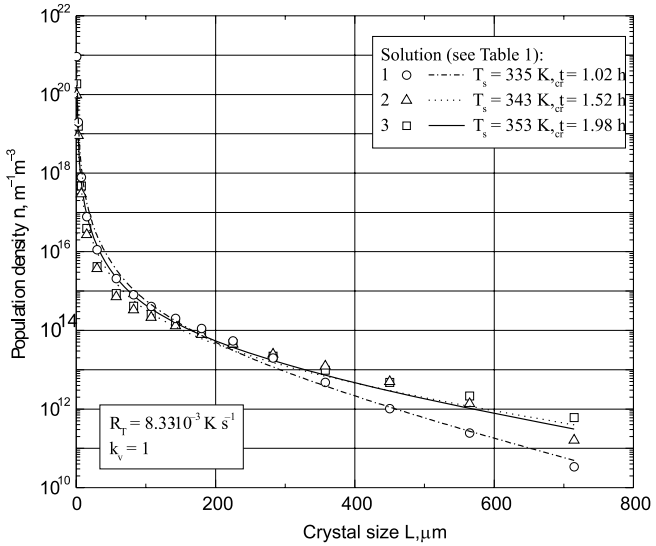

Figure 1. A comparison of population density distributions of L(+)-ascorbic acid crystals produced in a batch mode: points – experimental data, solid lines – values calculated with the use of Eq. (8) and data from Table 1 (the Rojkowski hyperbolic SDG model applied)

Crystal population balance equation for MSMPR crystallizer can be then rearranged to the form of Eq. (2)[32]:

$$-\frac{dn(L)}{n(L)} = \frac{dL}{G(L)\tau} + \frac{dG(L)}{G(L)} \tag{2}$$

After the assumption of some selected (empirical, semi-empirical or theoretical) form of G(L) dependency[33] an analytical solution (or its numerical approximation) of the resulting equation:

$$-\int_{n_0}^{n} \frac{dn}{n(L)} = \int_{0}^{L} \frac{dL}{G(L)\tau} + \int_{G_0}^{G} \frac{dG(L)}{G(L)} \tag{3}$$

is required. Eqs (2) and (3) can be, however, directly adopted for rough calculation of a substitute-G value in a batch crystallization process by a formal substitution of average residence time of crystal suspension, t (in continuous mode) with a batch crystallization time, t_{cr}, Eq. (4):

$$\tau \approx t_{cr} = \frac{T_{cr} - T_f}{R_T} + t_f \tag{4}$$

The t_{cr} value thus depends both on the properties of the initial solution introduced into a batch crystallizer ($T_{cr} = T_s - \Delta T_{max}$, $\Delta c_{max} = (dc/dT)_{eq}\Delta T_{max}$) and the technological process conditions (R_T, T_f, t_f). Considering the $T_{cr} = f(c_{LAA}, c_{MeOH}, c_{EtOH})$ dependency evaluated in the authors' paper[20], Eq. (4) can be presented in a more detailed form: $\tau \approx t_{cr} = f(c_{LAA}, c_{MeOH}, c_{EtOH}, T_f, R_T, t_f)$ – Eq. (5):

$$\tau \approx t_{cr} = \frac{2.932c_{LAA} + 0.671c_{MeOH} + 0.883c_{EtOH} + 174.78 - T_f}{R_T} + t_f \tag{5}$$

For a more precise estimation of growth kinetics in a batch process of LAA mass crystallization from water-alcohols mixture a Rojkowski hyperbolic SDG model – system of Eqs (6) and (7)[33, 34]:

$$G(L) = G_\infty - \left(\frac{G_\infty - G_0}{1 + aL}\right) = \frac{G_0 + aG_\infty L}{1 + aL} \tag{6}$$

$$n(L) = n_0 \exp\left[-\left(\frac{1}{\tau}\frac{G_\infty - G_0}{aG_\infty^2}\ln\left(\frac{aG_\infty L + G_0}{G_0}\right) + \frac{1}{\tau}\frac{L}{G_\infty} + \ln\left(\frac{G_0 + aG_\infty L}{(1+aL)G_0}\right)\right)\right] \tag{7}$$

was formally adopted. Eq. (7) is the solution of population balance, Eq. (3), for a continuous process mode after the selected G(L) – here Eq. (6) – function introduction. Its adjustment to the batch mode by a formal substitution of $\tau = t_{cr}$ (Eqs (4) and (5)) provides the form of Eq. (8) directly:

$$n(c_{LAA}, c_{MeOH}, c_{EtOH}, T_f, R_T, t_f, L) = n_0 \exp\left[-\left(\frac{1}{\left[\frac{2.932c_{LAA} + 0.671c_{MeOH} + 0.883c_{EtOH} + 174.78 - T_f}{R_T} + t_f\right]}\frac{G_\infty - G_0}{aG_\infty^2}\ln\left(\frac{aG_\infty L + G_0}{G_0}\right) + \frac{1}{\left[\frac{2.932c_{LAA} + 0.671c_{MeOH} + 0.883c_{EtOH} + 174.78 - T_f}{R_T} + t_f\right]}\frac{L}{G_\infty} + \ln\left(\frac{G_0 + aG_\infty L}{(1+aL)G_0}\right)\right)\right] \tag{8}$$

The resulting Eqs (7) or (8), originally evaluated from general population balance with the assumptions of a continuous MSMPR crystallizer, can be treated here as a convenient

Table 2. The kinetic parameter values of crystals growth in a batch process of L(+)-ascorbic acid crystallization (the SIG[27] and SDG kinetic models applied)

Model	Solution (see Table 1)	n_0	G_0	G^*, G_∞	a	R^2
		$m^{-1}m^{-3}$	m s^{-1}	m s^{-1}	m^{-1}	–
SIG[27]	1	$1.74 \cdot 10^{15}$	–	$1.74 \cdot 10^{-8}$	–	0.995
	2	$6.56 \cdot 10^{14}$	–	$1.41 \cdot 10^{-8}$	–	0.996
	3	$4.85 \cdot 10^{14}$	–	$1.43 \cdot 10^{-8}$	–	0.989
SDG (Eqs (6) – (8))	1	$2.36 \cdot 10^{25}$	$2.47 \cdot 10^{-12}$	$3.33 \cdot 10^{-8}$	4683	0.996
	2	$8.40 \cdot 10^{25}$	$4.29 \cdot 10^{-13}$	$4.50 \cdot 10^{-8}$	2611	0.989
	3	$1.05 \cdot 10^{29}$	$2.71 \cdot 10^{-14}$	$2.86 \cdot 10^{-8}$	3078	0.990

*The G value was calculated with the use of the SIG kinetic model (the linear course of lnn(L)) fitted statistically to the experimental population density data in the range of L > 100 μm only

mathematical tool for a more detailed description of „average, effective" kinetics in the batch system presenting both the curvature within the smallest size range (L < 100 μm) and the nearly straight course for the largest sizes (apparent compatibility with the McCabe's rule – called „*Bujakian behavior*"[35]).

Exemplary SDG calculations were performed for the experimental population density distributions corresponded to the cooling rate of $R_T = 8.33 \cdot 10^{-3}$ K s^{-1}. The regression procedure (the multiparameter nonlinear fitting of experimental n(L) data to Eq. (7) frame) was executed with the use of ORIGIN 6.2 software. The resulting values of kinetic parameters (n_0, G_0, G_∞, a) are presented in Table 2. In this Table there are also presented – for comparison purposes – the kinetic parameter values (n_0, G) calculated with the use of the most simplified SIG (size-independent growth) model (characterized by the linear course of n(L) dependency for a whole L range, including L < 100 μm).

Analyzing the data in Table 2 it can be concluded that the values of the maximal growth rate (G_∞) in a SDG model are higher than the corresponded G values from a SIG model (however of the same order of magnitude), which can be explained in terms of the intrinsic nonlinearity of a more flexible SDG model (apparent the linearity, however a slight curvature of the lnn(L) function for the largest size range in reality – contrary to a pure straight line in the simplest SIG model). As regards the minimal growth rate (G_0) parameter value it has been observed that it decreases (each time by one order of magnitude) with the increase of the batch crystallization time, which is graphically reflected by a more pronounced curvature in a lnn(L) function course within the smallest size range. Assuming the linear course of the lnn(L) function (the SIG model), for L = 0 an „*effective zero-size population density*", n_0, is obtained. However, using a more complex, thus a mathematically flexible SDG model – Eq. (7), one can predict, taking advantage of its nonlinear course within the smallest size range, a more precise (more realistic) value of „*zero-size population density*", n_0.

It must be strongly emphasized – once again – that these „average, effective" values of G_0 and G_∞ should also be interpreted only as the computationally convenient, conventional and strictly „formal" process parameters – without any grounded physical or theoretical-cognitive sense. These values can be, however, practically useful in design works or in the more precise engineering calculations, e.g. for the possible accurate prediction of the cumulative mass distribution, W(L), of product crystals, Eq. (9), or their specific surface area distribution, F(L), Eq. (10) under the assumed (however, experimentally verified) technological conditions:

$$W(L) = \frac{k_v \rho_s \int_0^L L^3 n(L) dL}{k_v \rho_s \int_0^\infty L^3 n(L) dL} \tag{9}$$

$$F(L) = \frac{k_F \int_0^L L^2 n(L) dL}{k_F \int_0^\infty L^2 n(L) dL} \tag{10}$$

The last parameter's distribution, F(L) – Eq. (10), is especially important in the design of the processes of modern advanced technologies, e.g. in the synthesis of pharmaceutical compounds (powders) in the complex reaction-crystallization processes or the precipitation of pigments with the use of expensive substrates, where mass crystallization operations are realized in a batch regime for the increase of the possibility of a precise process control facing a small production scale. Thus, the n(L) distributions used in Eqs (9) and (10), estimated on the basis of the simplest SIG kinetic model (assuming the linearity of lnn(L)) could produce some serious inaccuracies in the process calculations related to this, practically the most important in the present technical applications, range of the smallest L. This way the suggested correction (formal application of the SDG model equations for the description of the batch process kinetics) enables one to increase the computational precision in the complex design calculations. This way, formally correct but arduous, precise physical models, based on the systems of balance differential equations of parameters changed in time, requiring – during the elaboration and computations – some advanced mathematical methods, are not necessary. It should be also kept in mind that all these „average, effective" values of G[28] correspond to some hypothetical, entirely theoretical values of fixed, stabilized „average supersaturation", being in fact for a batch process conditions – contrary to the continuous mode – a dynamic parameter, dramatically changeable in time during the real process course.

Crystal habit, shape and size

Scanning microscope images (Figure 2a – c) present a product crystal population formed when the system is provided with a solution of c_{LAA} = 40, 45 and 50 mass %, resulting in batch crystallization time t_{cr} = 1.02, 1.52 and 1.98 h. These pictures confirm qualitatively the statistical distribution data and their kinetic interpretation presented above (see the values in Tables 1 and 2). With the increase of the initial concentration of L(+)-ascorbic acid from 40 to 50 mass %, critical super-cooling ΔT_{max} decreases from 29 to 18 K, which results in the advantageous increase of batch crystallization

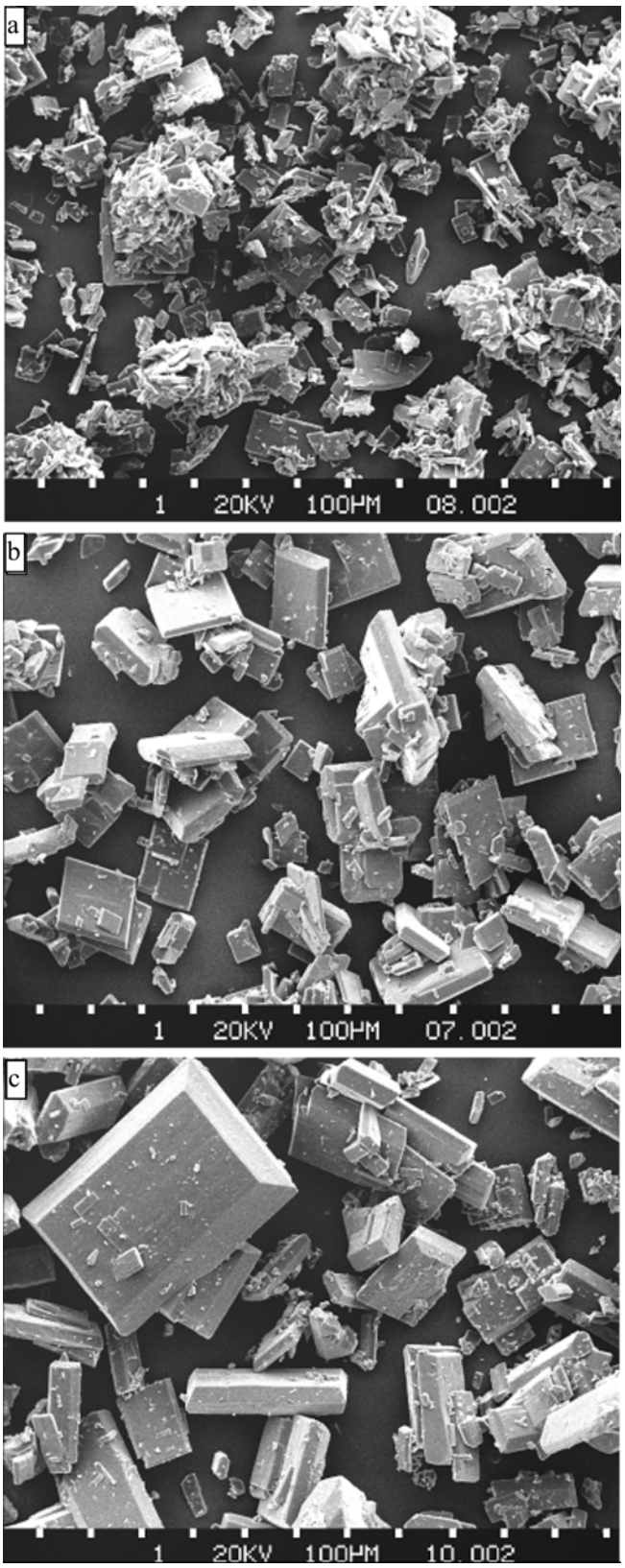

Figure 2. Scanning microscope images (magnification: 100x) of L(+)-ascorbic acid (LAA) crystals produced in the batch LAA-MeOH-EtOH-H_2O system (membrane cooling DT-type laboratory crystallizer): (a) test No. 1, (b) test No. 2, (c) test No. 3 – see the corresponding data in Tables 1 and 2.

time, tcr, from 1.02 to 1.98 h (the constant cooling rate assumed: $R_T = 8.33 \cdot 10^{-3}$ K s^{-1}). This way for higher c_{LAA} values the more convenient conditions of crystals growth are provided, resulting in the increase of mean crystal size L_m from 214 to 448 μm, while the CV parameter advantageously decreases from 62.2 to 31 % (see Table 1). All these effects are visible in Figure 2a – c, where larger particles dominate for c_{LAA} = 50 mass % compared to c_{LAA} = 40 and 45 mass %. However, proper interpretation of the kinetic data presented in Table 2 requires taking into account the agglomeration phenomena accompanying the main process course. In the (a) case some significant diversity in crystal size is observed, although the individual particles are relatively small, forming stable agglomerates. In the (b) case some larger crystals are observed while a decrease of fines and agglomerates is also visible. The largest individual crystals appear in the (c) case where the intensity of agglomeration effects is strongly reduced. Two effects are generally observed – the intrinsic kinetics of the growth of individual particles (final effects are the most visible in the (c)) case and agglomerates / aggregates creation (whose gffects are the most visible in the (a)) case. Both tendencies gradually change, however in opposite directions, which can be observed in these microscope images. Both the individual crystals and stable agglomerates / aggregates are counted the same in laser particle size analyzing, thus the apparently unexpected, practically identical values of $G_\infty = 2.86\text{-}4.50 \cdot 10^{-8}$ m s^{-1} are observed, representing a net effect of the intrinsic growth and agglomeration kinetics. The relatively high value of n_0 in the (c) case ($n_0 = 1.05 \cdot 10^{29}$ $m^{-1}m^{-3}$) compared to cases a – b (where $n_0 = 2.36\text{-}8.40 \cdot 10^{25}$ $m^{-1}m^{-3}$) results from the practical absence of agglomeration (except for a small number of fines firmly attached to the properly shaped parent crystals, practically not influencing their sizes), thus the occurrence of the smallest crystals in a free, not bounded form. In spite of agglomerates formation (case (a)), the difference in extreme sizes between the sparse free fines and the developed product crystals (aglomerates) is two-times higher (CV = 62.2%) compared to the (c) case (CV = 31.0% resulting from no agglomeration effects) where, moreover, this range moved towards larger sizes.

CONCLUSIONS

Technologically effective purification of the technical grade vitamin C is an important problem in pharmaceutical and food industry. Addition of methanol and ethanol - in various proportions – enables one to influence the process yield and the product quality (crystal size distribution, mean size, CV). Proper exploitation of these complex interrelations in engineering practice requires elaboration of a possibly precise kinetic model, directly predicting the population density course in respect to the initial composition of the batch mixture, as well as the technological parameters of the process (in a form of – for example – Eq. (8)). The Nývlt's conception of the batch kinetic data evaluation on the basis of a continuous MSMPR model frame incorporating the SDG effects was applied, resulting in a set of kinetic parameter values (Table 2). These data can be used, however, as the pure numerical values useful in various design calculations, e.g. in a more accurate prediction of the cumulative mass distribution or the specific surface area distribution under any process conditions. It should be, however, noted that only the coupled analysis of the population density data and electron microscope images enable one to make a correct interpretation of the kinetic data.

ACKNOWLEDGEMENTS

This work was supported by the Scientific Research Committee (Ministry of Science and Higher Education) under grant No. 3T09B 122 27.

Crystal size distributions of LAA were measured by means of the particle size analyzer COULTER LS-230 at the Institute of Inorganic Chemistry, Gliwice, Poland.

The images of the LAA crystals (scanning electron microscope JEOL-5800 LV) were made in Head of Materials Science Laboratory of the Institute of Materials Science and Applied Mechanics, Wrocław University of Technology, Wrocław, Poland.

NOMENCLATURE

a – parameter in the Rojkowski hyperbolic SDG model, m^{-1};
c – concentration, mass %;
CV – coefficient of variation (of crystal sizes), %;
c_{EtOH} – initial concentration of ethanol in a batch solution, mass %;
c_{LAA} – initial concentration of L(+)-ascorbic acid (LAA) in a batch solution, mass %;
c_{MeOH} – initial concentration of methanol in a batch solution, mass %;
Δc_{max} – critical, maximal supersaturation attainable in a given solution under specified technological conditions, mass %;
F – normalized specific surface area distribution;
G – linear growth rate of crystals, m s^{-1};
G_i – individual linear growth rate of i-th crystal, m s^{-1};
G_0 – minimal linear growth rate of crystals (growth rate of nuclei), m s^{-1};
G_∞ – maximal linear growth rate of crystals, m s^{-1};
k_v – volumetric shape factor of crystals;
k_F – surface shape factor of crystals;
L – crystal characteristic size, m;
L_i – mean size of i-th crystal fraction, m;
ΔL_i – size range width of i-th crystal fraction in Eq. (1), m;
L_m – mean size of crystal population, m;
m – mass, kg;
m_i – mass of i-th crystal fraction in Eq. (1), kg;
n – population density (number of crystals within the defined size range per unit volume of the suspension and per this size range width), $m^{-1}m^{-3}$;
n_i – population density of i-th crystal fraction in Eq. (1), $m^{-1}m^{-3}$;
n_0 – population density of nuclei (zero-size crystals), $m^{-1}m^{-3}$;
q_v – volumetric flow rate of suspension in a continuous mode, m^3s^{-1};
R – statistical correlation coefficient;
R_T – (linear) cooling rate, K s^{-1};
T – process temperature, K;
T_{cr} – temperature of spontaneous LAA nucleation, K;
T_f – final temperature of batch crystallization process, K;
T_s – LAA solubility temperature, K;
ΔT_{max} – critical, maximal value of super-cooling attainable in a given solution under the specified technological conditions, defined as $T_s - T_{cr}$, K;
t_{cr} – batch crystallization time, s;
t_f – time of stabilizaton of the resulting post-processing suspension at the final batch process temperature, s;
V – volume, m^3;
V_i – volume of the i-th crystal fraction in Eq. (1), m^3;
V_w – working volume of crystallizer, m^3;
W – normalized cumulative mass distribution (undersize);

Greek letters

ρ – crystal density, kg m^{-3};
τ – mean residence time of suspension, defined by V_w/q_v, s;

Abbreviations

CSD – Crystal Size Distribution;
DT – Draft Tube (crystallizer type);
EtOH – ethanol;
GRD – Growth Rate Dispersion;
LAA – L(+)-ascorbic acid (vitamin C);
MeOH – methanol;
MSMPR – Mixed Suspension Mixed Product Removal (crystallizer type);
SDG – Size-Dependent Growth;
SIG – Size-Independent Growth.

LITERATURE CITED

1. Boudrant, J. (1990). Microbial processes for ascorbic acid biosynthesis: a review. *Enzyme Microb.* Technol. 12, 322 – 329.

2. Davies, M. B., Austin, J. & Partridge, D. (1991). *Vitamin C: Its chemistry and biochemistry*. Cambridge, UK: The Royal Society of Chemistry.

3. Reichstein, T. & Grussner, A. (1934). A good synthesis of L-ascorbic acid (Vitamin C). *Helv. Chim. Acta* 17, 311 – 328.

4. Šnajdman, L. O. (1973). *Proizvodstvo vitaminov*. Moskva, Russia: Piščevaja promyšlennost.

5. Paul, E. L., Tung, H. H. & Midler M. (2005). Organic crystallization processes. *Powder Technol*. 150, 133 – 143. DOI: 10.1016/j.powtec.2004.11.040.

6. Matynia, A. & Wierzbowska, B. (1986). Solubility and nucleation of ascorbic acid in water. *Przem. Chem*. 65, 613 – 615.

7. Matynia, A. & Wierzbowska, B. (1986). The influence of some factors on the yield of ascorbic acid crystallization from aqueous solutions. *Przem. Chem*. 65, 672 – 674.

8. Matynia, A. & Wierzbowska, B. (1987). Studies on the quality of ascorbic acid crystals obtained from aqueous solutions. *Przem. Chem*. 66, 288 – 289.

9. Bodor, B., Halasz, S. & Vassanyi, I. (1993). Crystallization parameters influencing size, habit and purity of vitamin C. In: Proceedings of the 12th Symposium on Industrial Crystallization, Z. H. Rojkowski (Ed.) (pp. 4.065 – 4.070). Warsaw, Poland.

10. Bodor, B. & Dodony, I. (1995). Crystallization of vitamin C under different experimental conditions. *Hung. J. Ind. Chem*. 23, 289 – 291.

11. Bodor, B. & Lakatos, B.G. (1999). Crystal growth of L-ascorbic acid in programmed batch cooling crystallization. *Hung. J. Ind. Chem*. 27, 297 – 300.

12. Freitas, A.M.B. & Giulietti, M. (2002). Crystallization of L-ascorbic acid from aqueous solutions. In: Proceedings of the 15th Symposium on Industrial Crystallization, A. Chianese (Ed.) Vol. 1, No. 232. Sorrento, Italy.

13. Omar, W. & Ulrich, J. (2006). Effect of the addition of alcoholic miscible co-solvents on the properties of ascorbic

acid in its supersaturated aqueous solution. *Cryst. Res. Technol*. 41, 431 – 436. DOI: 10.1002/crat.200510601.

14. Omar, W. (2006). Effect of solvent composition on crystallization process of ascorbic acid. *Chem. Eng. Technol*. 29, 119 – 123. DOI: 10.1002/ceat.200500283.

15. Suprunov, N.A., Lymar, A.P., Varentsov, V.V., Streltsov, V.V. & Smirnov N.Ju. (1994). Linear growth rate of ascorbic acid crystals during crystallization from water – alcohol solutions. *Massov. Kristall*. 3, 45 – 50.

16. Matynia, A., Wierzbowska, B., Bechtold, Z. & Kozak, E. (1999). Nucleation of vitamin C. In: Proceedings of the 14th Symposium on Industrial Crystallization, CD-ROM No. 0090. Cambridge, UK: Inst. Chem. Eng.

17. Matynia, A., Wierzbowska, B. & Bechtold, Z. (1998). Kinetics of nucleation and crystal growth for L(+)-ascorbic acid in aqueous solution with methanol, ethanol or isopropanol. *Inż. Ap. Chem*. 37(6), 3 – 7.

18. Matynia, A., Wierzbowska, B. & Szewczyk, E. (2000). Crystal growth of L(+)-ascorbic acid in a batch crystallizer. *Pol. J. Chem. Technol*. 2(1), 14 – 18.

19. Matynia, A. & Wierzbowska, B. (1987). Obtaining crystalline vitamin C from water – methanol solutions. *Inż. Ap. Chem*. 26(4), 15 – 18.

20. Wierzbowska, B., Matynia, A., Piotrowski, K. & Koralewska, J. (2007). Solubility and nucleation in L(+)-ascorbic acid – methanol – ethanol – water system. *Chem. Eng. Proc*. 46, 351-359. DOI: 10.1016/j.cep.2006.07.005.

21. Piotrowski, K., Wierzbowska, B., Koralewska, J. & Matynia, A. (2006). Neural model of the vitamin C solubility in a four-compound miscible system: L(+)-ascorbic acid-methanol-ethanol-water. In: Proceedings of 17th International Congress of Chemical and Process Engineering CHISA, CD-ROM, No. 288. Prague, Czech Republic: Proc. Eng. Publisher.

22. Piotrowski, K., Wierzbowska, B., Koralewska, J. & Matynia, A. (2006). Influence of methanol and ethanol on vitamin C crystallization temperature – neural network model. *Pol. J. Chem. Technol*. 8(4), 23 – 26.

23. Matynia, A., Wierzbowska, B., Szewczyk, E. & Bechtold, Z. (2001). Growing of vitamin C crystals in the system: L(+)-ascorbic acid – methanol – ethanol – water. Inż. Ap. Chem. 40(5), 23 – 24.

24. Wierzbowska, B., Matynia, A., Ćwiertnia, E. & Bechtold, Z. (2004). Quality of vitamin C crystals in the L(+)-ascorbic acid-methanol-ethanol-water system. *Inż. Ap. Chem*. 43(4/5), 48 – 49.

25. Wierzbowska, B., Matynia, A., Bechtold, Z. & Małasińska, M. (2004). Crystallization capacity in the L(+)-ascorbic acid – methanol – ethanol – water system. *Inż. Chem. Proc*. 25, 1771 – 1776.

26. Wierzbowska, B., Koralewska, J., Matynia, A. & Piotrowski, K. (2006). Attempts to estimate the linear growth rate of vitamin C crystals. *Inż. Ap. Chem*. 45(4), 152 – 153.

27. Wierzbowska, B., Piotrowski, K., Koralewska, J. & Matynia, A. (2008). Growth kinetics of vitamin C in L(+)-ascorbic acid – methanol – ethanol – water system: size-independent growth model approach. *Chem. Biochem. Eng. Q*. 22 (in press).

28. Nývlt, J., Söhnel, O., Matuchová, M. & Broul, M. (1985). *The kinetics of industrial crystallization.* Prague, Czech Republic: Academia.

29. Garside, J., Mersmann, A., & Nývlt, J. (1990). *Measurement of crystal growth rate*. München, Germany: European Federation of Chemical Engineering – Working Party on Crystallization.

30. Mullin, J.W. (1992). *Crystallization*. Oxford, UK: Butterworth – Heinemann.

31. Rojkowski, Z. & Synowiec J. (1991). *Krystalizacja i krystalizatory*. Warsaw, Poland: WNT.

32. Randolph, A.D. & Larson, M.A. (1988). *Theory of particulate processes: analysis and techniques of continuous crystallization*. New York, USA: Academic Press.

33. Machej, K. & Piotrowski K. (2001). Review and comparision of kinetic equations for mass crystallization design purposes. *Inż. Ap. Chem*. 40(5), 17 – 19.

34. Rojkowski, Z. (1978). New hyperbolic empirical model of size dependent crystal growth. *Bulletin de L'Academie Polonaise des Sciences – Serie des sciences chimiques.* 26, 265 – 270.

35. Myerson, A.S. (1993). *Handbook of industrial crystallization*. Stoneham, MA, USA: Butterworth-Heinemann.